Antarctic Science 1 (3): 279–290 (1989)

The Antarctic drainage flow: implications for hemispheric flow on the Southern Hemisphere

IAN N. JAMES

Department of Meteorology, University of Reading, Reading RG6 2AU, UK

Abstract: An Ekman analysis of the surface drainage winds over a sloping ice surface is reported. Ekman pumping by the boundary layer leads to the formation of an upper tropospheric cyclonic vortex above the summit of the ice sheet. The strength and distribution of upper level vorticity is determined by the shape of the underlying ice sheet. The calculation is verified by comparison with the results from a multi-level primitive equation model of flow above an axisymmetric ice sheet. Both models predict that the surface drainage flow will die out on a timescale of a few days, while the upper vortex is predicted to be considerably stronger than observed. Various mechanisms which could lead to the depletion of upper level vorticity, and hence to the retention of a substantial drainage flow, are discussed. It is concluded that disruption of the polar vortex by decaying mid-latitude cyclones, and the consequent export of cyclonic vorticity to lower latitudes, is the most probable mechanism.

Received 9 March 1989, accepted 6 June 1989

Key words: Ekman layer, ice sheet, vorticity transport, vortex.

Introduction

The surface winds over the Antarctic ice sheet are the most persistent in the world. They are almost exclusively unidirectional and very steady (Schwerdtfeger 1984). Some of the strongest, as well as the most persistent winds on the Earth's surface have been observed at stations at the foot of the Antarctic coastal escarpment. It is clear that the surface wind pattern is intimately linked to the topography of the ice surface and to the continental scale surface inversion (as much as 30 K in the lowest few hundred metres of the atmosphere, Schwerdtfeger 1984) generated by intense cooling at the ice surface. The work of Ball (1960), Mahrt & Schwerdtfeger (1970), Parish (1982), Parish & Bromwich (1987) and others have established that boundary layer theories, which balance the downslope component of buoyancy with the Coriolis and friction forces, can account for the observed wind direction relative to the local ice slope.

Much less well observed is the flow in the middle troposphere above the Antarctic. The persistent horizontal divergence of flow in the boundary layer must be compensated by entrainment of air into the boundary layer, with subsidence and horizontal convergence in the middle troposphere. A schematic view of these processes is given in Fig. 1. Egger (1985) used an axisymmetric numerical model of drainage flow over the ice sheet to demonstrate such a meridional flow at upper levels. However, in his axisymmetric state, the drainage flow died away after a few days of integration. This result is not surprising; the drainage flow sets up a vortex over the pole at upper levels whose large-scale pressure gradients oppose the down slope buoyancy force. In the steady state, these two effects balance.

The aim of this paper is two-fold. First, the intensification of the polar vortex by the drainage flow will be considered. This subject has received rather scant attention in the literature, but may well be an important component of the large-scale circulation in the southern high latitudes. Second, the persistence of the observed drainage flow will be discussed. This persistence demands that the upper vortex should be weaker than suggested by axisymmetric models, with net export of cyclonic vorticity from the polar regions. This could be accomplished by local instabilities, by large-scale disturbances propagating from lower latitudes, or by local forcing due to the departure from axial symmetry of the Antarctic ice sheet. All such mechanisms involve relaxing the axial symmetry assumed in Egger (1985).

The approach followed is broadly parallel to that of Egger (1985). An Ekman boundary layer analysis is used to relate the surface drainage flow to the upper tropospheric vorticity. A nonlinear numerical model is described and some basic results with an axisymmetric version of the model are presented. Various mechanisms for maintaining the drainage flow are considered and some conclusions are discussed.

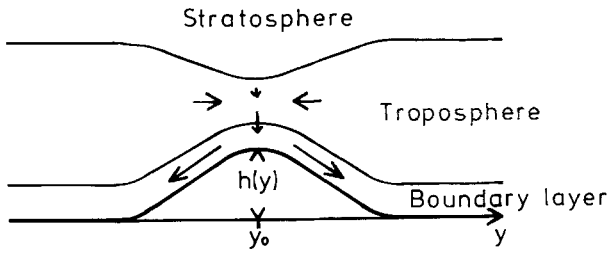

Fig. 1. Schematic illustration of the circulation induced by the Antarctic drainage flow. The nomenclature used in the analysis has been added.

https://doi.org/10.1017/S0954102089000404 Published online by Cambridge University Press

Ekman layer theory

In this section, a simple linear theory of the drainage flow is presented. The assumptions made are severe but serve to isolate some basic physical principles and to aid the interpretation of the numerical model results which will be presented in subsequent sections. The analysis extends that of Mahrt & Schwerdtfeger (1970) (see also appendix 4 of Schwerdtfeger (1984) although this analysis is marred by a number of typographical errors), and is closely related to the more rigorous approach given in Egger (1985). The objective here is to relate the upper tropospheric flow to the surface morphology and boundary layer characteristics.

For simplicity, consider the situation depicted in Fig. 1. The ice sheet is supposed to be infinite in the x-direction, so that its height varies only in the y-direction. A more realistic model of the ice sheet would possess axial symmetry (see below); while the resulting curvature of the ice sheet would alter the extent of the regions of ascent and descent over the ice sheet, it would not change the essential physics of the drainage flow. The height of the ice sheet, $h(y)$, falls smoothly to zero away from its maximum at $y = y_0$. It is supposed that the equilibrium potential temperature of the atmosphere is $\theta_0(z)$, while the potential temperature of the ice surface is maintained at $\theta_0(z) - \Delta\theta$. The slope of the ice surface is supposed always to be small, so that local co-ordinates parallel to the ice surface can be considered. This is realistic for Antarctica; the ice slope, h_y, is generally of the order of 10^{-3} except at its edge. In the steep and rugged orography of the ice margin, the present analysis is inappropriate. Finally, there may be large-scale horizontal pressure gradients in the region of the ice sheet. A geostrophic wind of u_g is supposed to blow parallel to the x-axis; it is assumed by symmetry that the y-component of the geostrophic wind is zero. With all these assumptions, the primitive equations for the flow can be written:

$$\frac{Du}{Dt} - fv = (Ku_z)_z \tag{1}$$

$$\frac{Dv}{Dt} + f(u - u_g) = (Kv_z)_z - g\frac{(\theta - \theta_0)}{\theta_0}h_y \tag{2}$$

where the second term on the right hand side of equation (2) represents the downslope component of the buoyancy force. K is a vertical diffusion coefficient and will be taken to be constant. This is clearly a poor approximation made only for simplicity. The question of parametrizing a highly stably stratified boundary layer is a complex and poorly understood problem which will not be pursued in this paper. The thermodynamic equation is of the form:

$$\frac{D\theta}{Dt} + \frac{\theta_0 N^2}{g}w = \frac{(\theta_0 - \theta)}{\tau} + (K\theta_z)_z. \tag{3}$$

$N = (g\partial \ln \theta_0/\partial z)^{1/2}$ is the Brunt-Väisälä frequency and will be used to measure static stability. The first term on the right hand side represents the tendency of the undisturbed atmosphere to relax towards the radiative equilibrium profile $\theta_0(z)$ on a timescale τ in the absence of boundary fluxes of heat. These heat fluxes are parametrized by $K\theta_z$.

Equations (1)–(3) are linearized about the state $u = v = 0$, $\theta = \theta_0$; only the steady solutions will be considered at present, so that the linearized boundary layer equations can be expressed:

$$-fv = Ku_{zz}, \tag{4}$$

$$f(u - u_g) = Kv_{zz} - g\frac{(\theta - \theta_0)}{\theta_0}h_y, \tag{5}$$

$$K\theta_{zz} = \frac{\theta_0 N^2}{g}h_y v + \frac{(\theta - \theta_0)}{\tau}. \tag{6}$$

The thermodynamic equation can be solved separately from the dynamic equations for cases of interest. Note that it is only coupled to the remainder of the system through the downslope advection term. The ratio of the first and second terms on the right hand side of equation (6) is typically

$$\frac{v}{v_R} \sim \frac{\theta_0 N^2 h_y \tau}{g\Delta\theta}v \tag{7}$$

near the surface, and smaller in the interior as $\theta \to \theta_0$. Taking $\tau = 5$ days, $h_y = 10^{-3}$ and $\Delta\theta = 30$ K yields $v_R = 19.2$ m s^{-1}. As we shall see, the downslope component of the wind rarely exceeds 1–2 m s^{-1} for reasonable parameters, and so the radiative relaxation term in equation (6) must form the dominant balance with the diffusion term. Under these circumstances, the vertical scale of the potential temperature variation will be sufficiently rapid in a surface boundary layer that diffusion balances the radiative tendencies. Physically, this approximation implies that air advected downslope in the boundary layer is essentially always in radiative equilibrium with the overlying layers of air; among other things, it implies that the boundary layer structure should be independent of N. In a more realistic model with $K = K(N)$, this would no longer be true; nevertheless, the thermodynamic and momentum equations would only be rather weakly coupled via the variation of K. The solution of (6) is

$$\theta = \theta_0 - \Delta\theta \exp\left(\frac{-z}{H_I}\right), \qquad H_I = (K\tau)^{1/2}. \tag{8}$$

For $\tau = 5$ days and $K = 10$ m^2 s^{-1}, H_I is around 2 km. This is considerably thicker than the inversion depth observed over the Antarctic plateau; a more realistic profile could be generated if K were to be a decreasing function of N. Such behaviour is physically plausible but its implementation would be entirely heuristic.

This solution for thermal structure of the boundary layer is substituted into the downslope momentum equation:

$$Kv_{zz} = f(u - u_g) + bh_y \exp\left(\frac{-z}{H_I}\right). \tag{9}$$

Here, $b = g\Delta\theta/\theta_0$ measures the inversion strength in terms of the buoyancy deficit at the surface. Equations (5) and (9) can

https://doi.org/10.1017/S0954102089000404 Published online by Cambridge University Press

be solved straightforwardly, using standard Ekman layer analysis. It is convenient to define the complex velocity

$$U = u + iv \tag{10}$$

so that (5) and (9) can be combined as:

$$U_{zz} - i\frac{f}{K}U = i\frac{f}{K}U_g + i\frac{b}{K}h_y e^{-z/H_I} \tag{11}$$

which has a particular integral:

$$U_1 = U_g + \frac{ih_y H_I^2}{(K - ifH_I^2)}e^{-z/H_I}. \tag{12}$$

The complementary function is:

$$U_0 = Ce^{-z/H_E}e^{-iz/H_E} + De^{z/H_E}e^{iz/H_E}, \tag{13}$$

where C and D are complex constants. As $z \to \infty$, $u = u_g$ and $v = 0$; hence $D = 0$. $H_E = (2K/f)^{1/2}$ is the classical Ekman layer scale height; for K = 10 m^2 s^{-1} H_E is 380 m, considerably smaller than H_I. Combining (12), (13) and breaking into real and imaginary parts, the general solution of the boundary layer equations is:

$$u = u_g + e^{-z/H_E}\left(C_1\cos\left(\frac{z}{H_E}\right) + C_2\sin\left(\frac{z}{H_E}\right)\right) - \frac{fbh_y H_I^4}{(K^2 + f^2H_I^4)}e^{-z/H_I}, \tag{14a}$$

$$v = e^{-z/H_E}\left(C_2\cos\left(\frac{z}{H_E}\right) + C_1\sin\left(\frac{z}{H_E}\right)\right) + \frac{Kbh_y H_I^4}{(K^2 + f^2H_I^4)}e^{-z/H_I}, \tag{14b}$$

where C_1 and C_2 are real constants whose values are determined from the boundary conditions $u = v = 0$ when $z = 0$. The full solution satisfying these boundary conditions is:

$$u = u_g + e^{-z/H_E}\left((u_B - u_g)\cos\left(\frac{z}{H_E}\right) + \frac{u_B}{f\tau}\sin\left(\frac{z}{H_E}\right)\right) - u_B e^{-z/H_I}, \tag{15a}$$

$$v = e^{-z/H_E}\left(\frac{u_B}{f\tau}\cos\left(\frac{z}{H_E}\right) + (u_B - u_g)\sin\left(\frac{z}{H_E}\right)\right) + \frac{u_B}{f\tau}e^{-z/H_I}, \tag{15b}$$

where

$$u_B = \frac{fbh_y H_I^4}{K^2 + f^2H_I^4} \tag{16}$$

is a constant with the dimensions of velocity. Again, substituting numerical values for K = 10 m^2 s^{-1} gives u_B = 7.6 ms^{-1}. Note that the first term on the denominator of (16) is very small compared with the second, so that $u_B = b\,h_y/f$ to a good approximation. The strength of the downslope wind is therefore independent not only of K but also of τ; these parameters serve just to determine the vertical scale of the boundary layer and the mass flux which it carries.

Fig. 2 shows profiles of u and v for various values of u_g. When $u_g = 0$, the meridional wind is downslope, with a maximum value of 2.5 ms^{-1} (confirming the neglect of downslope thermal advection in equation (7)). Easterly zonal winds, up to 5.7 ms^{-1}, develop in the boundary layer as a consequence. The surface wind direction is close to 45° to the slope. As u_g is increased, the downslope wind (and mass flux) decreases; for $u_g = u_B$ the downslope component is very small and the zonal wind increases monotonically from 0 to u_g through the boundary layer. The lack of downslope wind in this case is readily understood; the meridional pressure gradients in balance with u_g oppose the downslope wind in the boundary layer and virtually remove it when $u_g = u_B$.

At this point, the argument is carried a stage further than in Mahrt & Schwerdtfeger (1970) and Egger (1985). In the absence of other dynamic effects, u_g is determined by Ekman pumping out of the boundary layer. Such pumping will

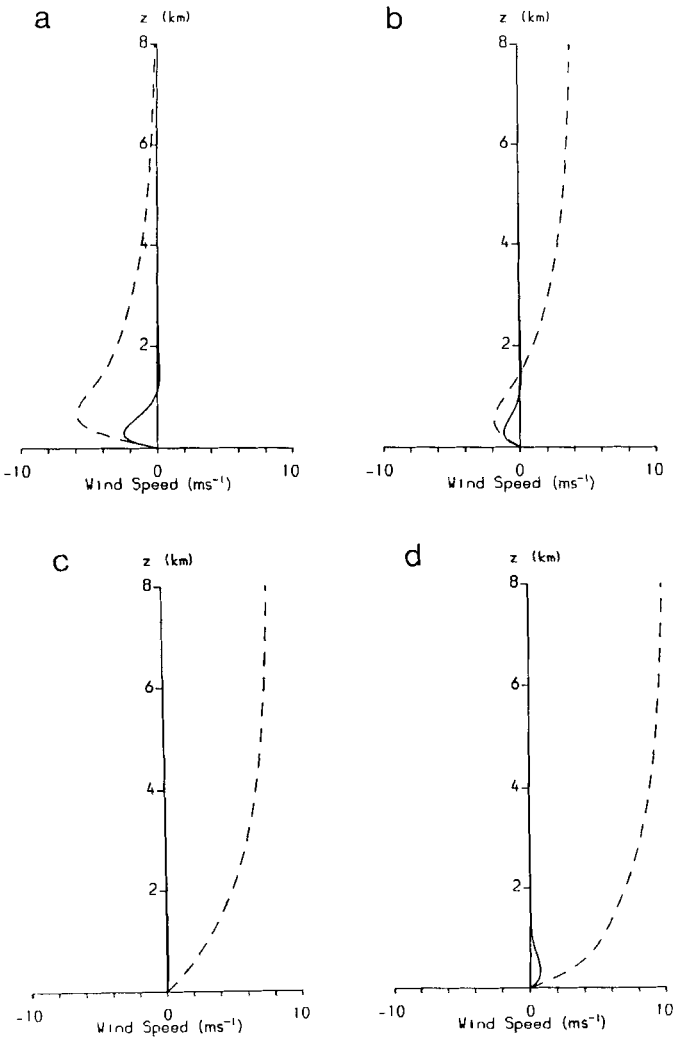

Fig. 2. Profiles with height z of downslope wind (——) and cross slope wind (– – –) calculated using equation (15). Parameter values were: K = 10 m^2 s^{-2}, τ = 5 days, $\Delta\theta$ = 30 K and $h_y = 10^{-3}$, giving u_B = 7.6 ms^{-1}. **a.** $u_g = 0$, **b.** u_g = 4 ms^{-1}, **c.** u_g = 7.6 ms^{-1} and **d.** u_g = 10 ms^{-1}.

https://doi.org/10.1017/S0954102089000404 Published online by Cambridge University Press

generate relative vorticity by vortex stretching in the troposphere above the boundary layer; when axial symmetry is imposed, a steady state will be reached when u is such that the mass flux out of the boundary layer is zero. From equation (15), the horizontal divergence in the boundary layer is:

$$\frac{\partial v}{\partial y} = -\frac{\partial u_B}{\partial y}\left\{\frac{e^{-z/H_E}}{f\tau}\cos\left(\frac{z}{H_E}\right) + e^{-z/H_E}\sin\left(\frac{z}{H_E}\right) + \frac{e^{-z/H_I}}{f\tau}\right\} + \frac{\partial u_g}{\partial y}e^{-z/H_E}\sin\left(\frac{z}{H_E}\right), \quad (17)$$

($\partial u/\partial x = 0$ by symmetry). The vertical velocity at the top of the boundary layer is therefore

$$w_\infty = \int_0^\infty \frac{\partial w}{\partial z}dz = \frac{\partial u_B}{\partial y}\left\{\frac{H_E}{2f\tau} + \frac{H_E}{2} + \frac{H_I}{f\tau}\right\} + \frac{\partial u_g}{\partial y}\frac{H_E}{2}. \quad (18)$$

In a steady state, w_∞ must vanish (i.e., we demand that there is no vortex stretching in the mid-troposphere): in this case, the geostrophic vorticity in the mid troposphere must be related to the shape of the ice surface by:

$$\xi_g = \frac{\partial u_g}{\partial y} = -\frac{bh_{yy}}{f}\left\{1 + \left(\frac{2}{f\tau}\right)^{1/2} + \frac{1}{f\tau}\right\}. \quad (19)$$

When $f\tau$ is large, which is reasonable for most situations, equation (19) can be simplified yet further to give $\xi_g \simeq -bh_{yy}/f$ or $u_g \simeq -u_B$. In other words, the steady state is reached when the vertically averaged downslope component of the wind is zero.

In conclusion, the theory of this section suggests that the strength and direction of the drainage wind is rather insensitive to the vertical diffusion parameter and radiative relaxation rates assumed. So, in view of the *ad hoc* nature of these parametrizations, the theory is encouragingly robust. The steady state flow in the upper troposphere is related mainly to the shape of the ice surface and only very weakly to the details of the parametrizations; of course the rate at which this steady state is approached depends directly on the assumed values of K and τ. Cyclonic vorticity will be generated over the summit of the ice sheet, where h_{yy} is mainly negative, and anticylonic vorticity around its margin where h_{yy} is positive. The maximum zonal winds above the boundary layer will coincide with the inflexion point where $h_{yy} = 0$. Thus, a cyclonic vortex will be centred above the ice sheet.

Numerical model

The theory presented in the previous section required a large number of assumptions, many of which only roughly hold. In the remainder of this paper, the arguments will be based on the results of numerical simulations of the drainage flow. The model still makes use of a very simple parametrization of boundary layer fluxes and radiative forcing, but makes fewer approximations to the dynamics of the flow; it is therefore a theoretical tool intermediate in complexity between the simple theory of the previous section and complex simulations such as those of a high resolution general circulation model.

The model employed is a version of the Reading spectral model (Hoskins & Simmons 1975); it integrates the primitive equations using the spectral transform method in the horizontal and second order finite differences in the vertical, with $\sigma = p/p^*$ (p^* being the surface pressure) as vertical co-ordinate. The numerical scheme was designed to conserve energy and angular momentum. The usefulness of a σ co-ordinate model when a high ice sheet is present is obvious. The vertical grid was stretched to allow high vertical resolution in the boundary layer and coarser resolution towards the top of the model. It proved convenient to define the vertical grid by the function:

$$\sigma_i = \frac{r(i/N)}{1 + (r-1)(i/N)}, \quad i = 0 \text{ to } N. \quad (20)$$

Here, r is the ratio of the gridlength near the surface, where $\sigma = 1$, to the average gridlength, while N represents the number of levels. r was chosen so that there were around two gridlengths in the Ekman depth. The model was generally run with 15 levels in the vertical with triangular truncation at wave number 42 in the horizontal. Many of the calculations were carried out using an axisymmetric version of the model; this was simply and economically achieved without reprogramming by assuming 40-fold symmetry in the zonal direction. The model was run in a form which assumed symmetry about the equator; for conciseness, results for just one hemisphere will be presented.

The thermodynamic equation may be written:

$$\frac{D\theta}{Dt} = \frac{\theta_0 - \theta}{\tau} + \frac{g^2K}{R^2T_0^2}\frac{\partial^2\theta}{\partial\sigma^2} \quad (21)$$

where $\theta_0(p)$ is an equilibrium profile of potential temperature. It was chosen so that N^2 was constant at 1.3×10^{-4} s^{-2} in the troposphere (below 30 kPa) and 4×10^{-4} s^{-2} in the stratosphere; θ_0 was constant on pressure surfaces. T_0 is some standard surface temperature. Other parameters have the same meaning as in the previous section. The usual form of the vorticity and divergence equations was assumed, except that a similar vertical diffusion term was included. The lower boundary condition was $u = v = 0$ together with $\theta = \theta_0 - \Delta\theta$ at $\sigma = 1$.

An ice sheet was introduced in the form of an axisymmetric dome centred on the pole. Its height (see Fig. 3) was given by:

$$h(\phi) = h_0\left\{2 - \tanh\left[\frac{(\phi - \phi_0)}{\Delta\phi}\right]\right\}, \quad (22)$$

where h_0 is the maximum height of the ice sheet, ϕ is latitude, ϕ_0 is the edge of the plateau (generally taken to be 70°S) and Δ determines the maximum slope of the ice surface. $\Delta\phi$ was generally assumed to be 5°. Various numerical problems were avoided by the use of this smooth orography with its continuous gradient, although a more realistic model of the

https://doi.org/10.1017/S0954102089000404 Published online by Cambridge University Press

Antarctic would have the slope increasing monotonically to the coast where it would discontinuously change to zero.

The model used a semi-implicit time stepping scheme in order that the time steps may be large compared to the period of high frequency gravity waves without numerical instability. In fact, the vertical diffusion term with the stretched grid introduced a very stringent limitation on the timestep. For stability, the timestep

$$\Delta t < \frac{\Delta z^2}{3K} = \frac{(RT_0 \Delta\sigma/g)^2}{3K}, \tag{23}$$

where Δz (or $\Delta\sigma$) is interpreted as the minimum gridspacing, just above the surface. If it be required that the smallest vertical gridspacing be some fraction $1/r$ of the Ekman depth H_E, then

$$\Delta t < \frac{2}{3r^2 f}. \tag{24}$$

For $r = 2$, Δt must be less than 1200 s while for $r = 3$ it must be less than 500 s. For comparison, an explicit time scheme would be limited to $\Delta t < 480$ s by the fastest gravity waves, while the semi-implicit scheme without vertical diffusion would be limited merely by the usual Courant-Friedrich condition based on the largest wind speed, implying $\Delta t <$ 7000 s. While the limitation implied by equation (24) may be lessened by the use of an implicit form of the vertical diffusion term, it will still be necessary to use a very short timestep if one requires an accurate simulation of the evolution of the Ekman layer.

The initial state for the integrations was a motionless stably stratified atmosphere with $\theta = \theta_0$. Cooling at the surface set up a thermal boundary layer as given by equation (8). Where the surface was sloping, this cold boundary layer began to drain downwards, setting up the type of Ekman layer structure described in the previous section. The resulting secondary circulations generated upper level vorticity, reducing the drainage flow until a steady state was achieved. This required around 10 days of integration; by this time the drainage downslope wind component was less than 1 ms^{-1}.

Experiments with an idealized Antarctic continent

Results are first presented for an axisymmetric continent of Antarctica with a maximum height of 3000 m, whose profile is given by equation (22). The initial state consisted of a motionless, stably stratified atmosphere, so that temperature was constant on isobaric surfaces. A surface temperature which was 30 K lower than the ambient air at all latitudes was prescribed. No mid-latitude temperature gradients were forced, so that the atmosphere would remain motionless in the absence of any surface slope. It was checked that the program would actually retain a motionless atmosphere in these circumstances.

Fig. 3 shows a sequence of the mean meridional streamfunction and the mean zonal wind as the boundary layer developed. During the first few hours of the integration, a strong downslope wind developed as the surface inversion was established. At the lowest model level, it reached a maximum value of nearly 7 ms^{-1} about 10 hours from the start of the integration. The zonal component of wind developed just a little more slowly, but reached a maximum of 8 ms^{-1} easterly two hours or so later. At this stage, the flow profile was qualitatively similar to the analytic profile discussed in the last section. The surface wind made an angle of about 45° to the slope line, while the zonal winds above the boundary layer were still very light. Note that, even at this stage, the downslope component of wind was small compared with v_g, defined in equation (7), justifying the neglect of downslope potential temperature advection in the linear Ekman analysis. By 12 hours, shown in Fig. 3a, westerly zonal wind began to develop in the upper troposphere. A narrow jet ran around the edge of the plateau. As will be shown later, the maximum cyclonic vorticity associated with the upper jet was located close to the latitude where h_{yy} is most negative, as predicted by equation (19).

After 12 hours, the low level winds began to decline, while the jet at upper levels intensified. This decline was more or less steady, though with small fluctuations which may indicate some weak inertial oscillations with a period of around 12 hours. By day 6, shown in Fig. 3b, the maximum downslope wind had been reduced to 3 ms^{-1} and was still declining steadily. At the same time, the westerlies in the upper troposphere had reached a maximum of 7 ms^{-1}. The intensification of the upper tropospheric jet continued throughout the run, while the low level winds declined steadily. By day 30, the downslope wind component was 0.6 ms^{-1} and appeared to be steady at this value; the upper jet was 12 ms^{-1}, a value comparable to u_B for this continent (see equation (16)). Thus the drainage flow in the steady state was extremely weak, providing just enough circulation to maintain the atmosphere slightly away from radiative equilibrium.

The development of the boundary layer and the upper jet is just as predicted by the Ekman theory. The assumptions made in the Ekman analysis are justified. But the primitive equation model couples the boundary layer to a less schematic representation of the middle and upper tropospheric flow. Nevertheless, the development of a vortex over the plateau is predicted by the more complex model. The position and strength of the vortex are related to the morphology of the underlying ice sheet.

The model barely resolves the boundary layer structure. Comparison of a number of runs in which the vertical diffusion parameter was varied suggest that the poor resolution near the surface did not affect the downslope flow very much. The maximum drainage wind achieved was fairly insensitive to the vertical diffusion coefficient K, a result predicted by the Ekman analysis. Undoubtedly, at lower values of K, the boundary layer was artificially thickened

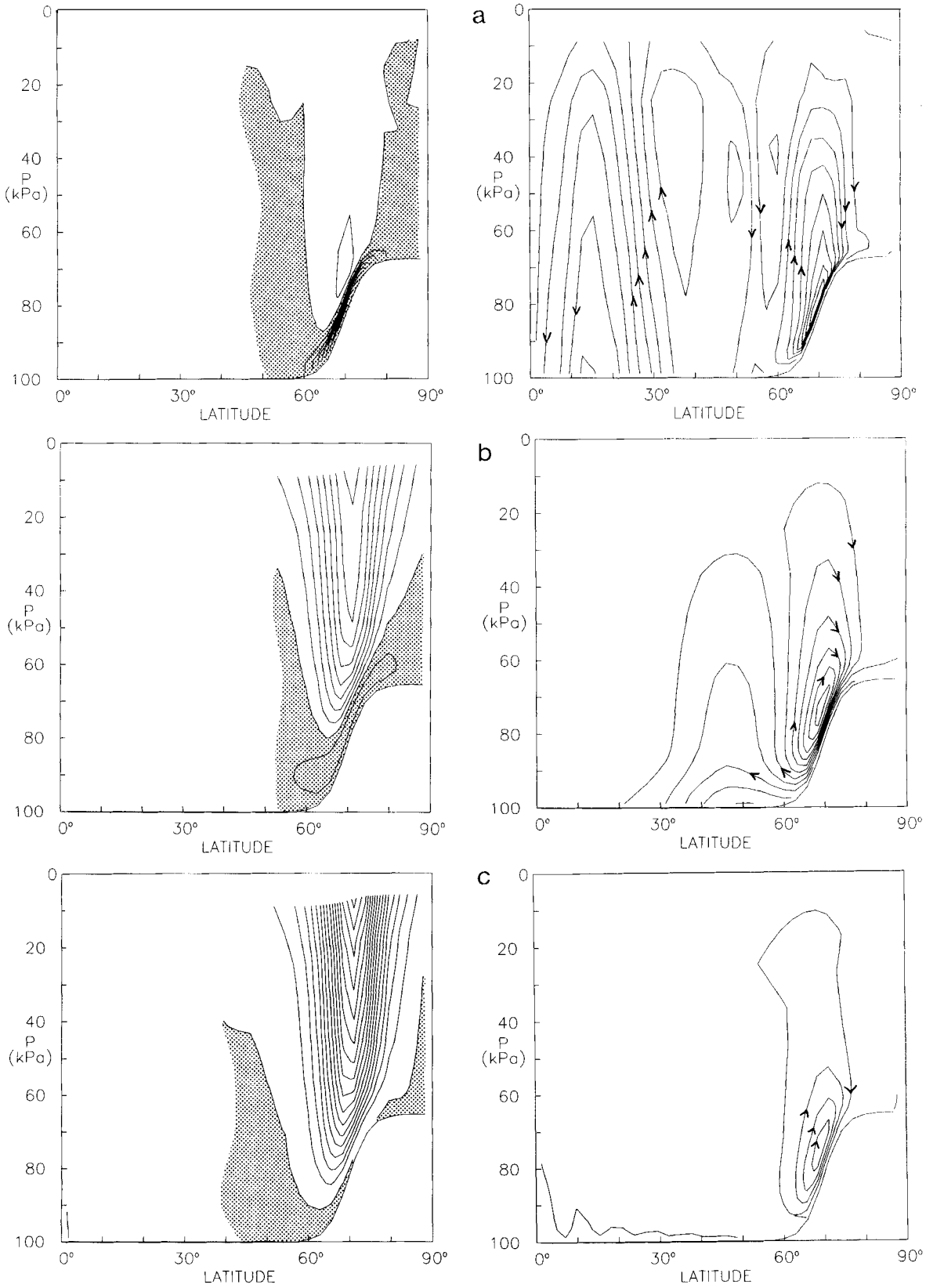

Fig. 3. The evolution of the drainage circulation over Antarctica (poleward of 60°) predicted by the primitive equation model. On the left are contours of zonal wind (contour interval 1 ms^{-1}, easterlies shaded) and on the right contours of meridional streamfunction (contour interval 250 Pa ms^{-1}). Parameter settings are defined in the text; h_0 was 3000 m. **a.** day 0.5, **b.** day 5.0, and **c.** day 30.

https://doi.org/10.1017/S0954102089000404 Published online by Cambridge University Press

by the excessive vertical grid spacing near the ground, and so the mass flux it carried was artificially large. The weak dependence of u_B on K inferred from the runs is probably a numerical result arising from the poor resolution of the boundary layer at small K. A severe computational penalty was incurred by decreasing the vertical spacing of the model levels near the surface, with the maximum timestep for which computational stability was guaranteed becoming extremely short.

We now consider a sequence of runs in which the height of the summit of the ice sheet took different values. All runs took $K = 10\ \mathrm{m^2 s^{-1}}$, $\Delta\theta = 30\ \mathrm{K}$, $N^2 = 1.3 \times 10^{-4}\ \mathrm{s^{-2}}$ and $\tau = 5$ days. As a check on the model, a control run with $h_0 = 0$ was carried out. This developed a stably stratified thermal boundary layer, as described by equation (8), but settled down to a steady state which was motionless on a timescale τ. Fig. 4 shows pressure-latitude cross-sections of the relative vorticity ξ for a sequence of runs with various h_0 at day 30 of the integrations. At this time, the runs were all close to a steady state. The integration was carried further in a few cases, and revealed some further slight adjustment of ξ. The majority of runs were terminated at day 30 in the interests of economy. Poleward of the inflexion point in the surface elevation, at latitude 70°, cyclonic vorticity developed, while weaker

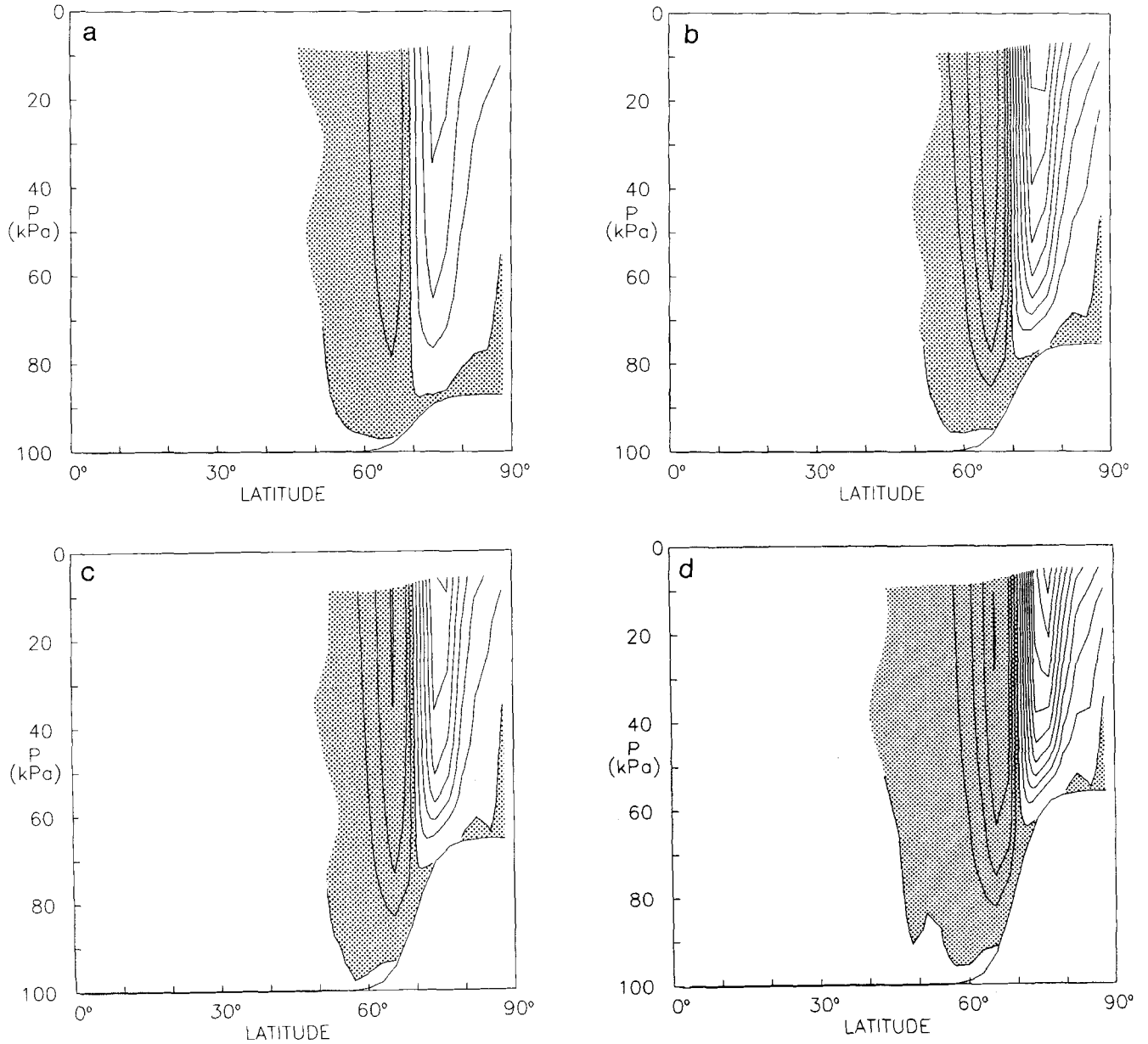

Fig. 4. Relative vorticity at day 30 from a series of primitive equation integrations using different ice sheet summit elevations h_0. **a.** $h_0 = 1000$ m, **b.** $h_0 = 2000$ m, **c.** $h_0 = 3000$ m and **d.** $h_0 = 4000$ m. Contour interval is $1.8 \times 10^{-6}\ \mathrm{s^{-1}}$ for a and b, $3.6 \times 10^{-6}\ \mathrm{s^{-1}}$ for c and d. Anticyclonic values are shaded.

https://doi.org/10.1017/S0954102089000404 Published online by Cambridge University Press

anticyclonic vorticity was seen equatorward of the inflexion point. Unlike the predictions of the Ekman theory, the relative vorticity was not antisymmetric about 70°. Such a lack of symmetry is expected as a consequence of the curvature of the ice sheet; the theory was restricted to an infinite straight ridge. But the broad patterns are in good qualitative agreement with equation (19).

In all the runs carried out, the same final pattern was achieved. The pressure gradients associated with the strong polar vortex choked off the surface downslope wind. This is in disagreement with observations, which suggest that the downslope winds are a permanent (although possibly fluctuating) feature of the Antarctic flow regime.

Mechanisms for maintaining the drainage flow

In order to account for the observed persistence of the surface drainage flow, it is necessary to identify mechanisms which could remove cyclonic vorticity from above the plateau. This might be accomplished either by the dissipation of vorticity locally, or by the transport of vorticity to lower latitudes. In either case, all mechanisms to be considered arise from the breakdown of the axisymmetric assumptions made in earlier sections.

Quasi-geostrophic theory enables the relationship between the meridional circulation and the various eddy and frictional forcings to be described, at least qualitatively. At the level of the quasi-geostrophic approximation, the zonal momentum equation is written:

$$[u]_t = f[v] - [u^* v^*]_y - F, \tag{25}$$

where [ ] denotes zonal mean and * denotes deviations from the zonal mean. F is a friction term, generally supposed to take the same sign as $[u]$. The thermodynamic equation may be written in the form:

$$[T]_t = -s[w] - [v^* T^*]_y + Q, \tag{26}$$

where s is a (positive) measure of static stability, w is a pseudo-vertical velocity $-H D \ln p/D t$ (H being the pressure scale height), and Q is a diabatic heating rate. Equations (25) and (26) are linked by the thermal wind equation:

$$[u]_z = -\frac{R}{fH}[T]_y \tag{27}$$

z being the pseudo-height $H \ln(p_0/p)$. Defining a meridional streamfunction ψ such that

$$[v] = -\frac{\partial \psi}{\partial z}, \qquad [w] = \frac{\partial \psi}{\partial y}, \tag{28}$$

the time dependent terms can be eliminated between (25) and (26) using thermal wind balance (27) to give:

$$\psi_{yy} + \frac{f^2 H}{sR}\psi_{zz} = -\left(Q_y - [v^* T^*]_{yy} - \frac{fH}{R}[u^* v^*]_{yz} - \frac{fH}{R}F_z\right). \tag{29}$$

This balance condition is an elliptic equation in ψ; negative source terms on the right hand side are associated with maxima in ψ and hence with a thermally direct meridional circulation, with ascent at low latitudes and descent at higher latitudes. The drainage flow will tend to be enhanced by such source terms and attenuated by positive source terms.

Radiation of Rossby waves

Antarctica is far from axisymmetric about the Earth's rotation axis; its centre is displaced some 10° of latitude from the geographical pole, and its shape is more complex than a simple dome. Parcels of air passing over the continent will experience low frequency forcing due to orographic and thermal effects which will project largely onto large-scale, low frequency balanced Rossby wave motions.

James (1988) discussed the forcing of Rossby waves by Antarctica. For present purposes, the crucial quantity is the meridional group velocity of Rossby waves. In the quasi-geostrophic framework, this is given by

$$c_y = \frac{2[q]_y kl}{(k^2 + l^2)^2} \tag{30}$$

where $[q]_y$ is the poleward gradient of quasi-geostrophic potential vorticity, k is the zonal wave number and l the meridional wave number. The latter is given by

$$l = \pm\left(\frac{[q]_y}{[u] - c} - k^2\right)^{1/2}, \tag{31}$$

c being the zonal phase speed of the waves. From equation (30), it will be seen that the negative root corresponds to equatorward group velocity. At high latitudes, where $[q]_y$ becomes small, only waves with the lowest zonal wave numbers k can propagate; smaller scale disturbances will be evanescent away from the continent. The poleward momentum flux is related to the amplitude of the forced Rossby waves A by:

$$[u^* v^*] = -\frac{kl}{2}|A|^2. \tag{32}$$

For waves forced by Antarctica and propagating equatorwards (i.e., $l \leq 0$), the momentum flux will be polewards. In terms of equation (28), the large values of $[u^* v^*]$ at upper levels and high latitudes will give positive source terms, and hence induce indirect circulations at high latitudes.

It is concluded that Rossby waves radiating equatorwards from Antarctica will tend to accelerate westerlies at high latitudes. Thus they will tend to inhibit the drainage flow further. Calculations with a three-dimensional version of the primitive equation model used above confirm this sign, but also show that the effect is quite small. Since both k and A in equation (32) will be small, this result might have been expected.

https://doi.org/10.1017/S0954102089000404 Published online by Cambridge University Press

Local baroclinic instability

The westerly jet predicted in the axisymmetric calculations may, in principle, be subject to baroclinic instability, although the slope of the plateau edge will introduce important modifications (Mechoso 1980). The stability of the zonal mean flow shown in Fig. 3c to wave-like normal mode perturbations of various zonal wave number was tested with a numerical solution of the eigenvalue problem generated by linearizing the full primitive equations about that wind and temperature field. The method which has been used extensively at Reading (e.g. James & Hoskins 1985, James & Gray 1986, MacVean & James 1986), was first described by Wyatt (1981). It enables the growth rate, phase speed and meridional structure of unstable disturbances of specified zonal wave number to be calculated. For the wave number 42 resolution needed to represent the Antarctic slope adequately, it is necessary to determine the eigenvalues and eigenvectors of a 966 × 966 matrix of complex coefficients. Such a large problem required several hours of computer time on the CRAY XMP computer at the Rutherford Appleton Laboratory. Higher resolution is not feasible with the current generation of supercomputers. However, it is believed that the current resolution is adequate, certainly in the horizontal, since the structure of the eigenmodes is well resolved. The vertical resolution of the model is undoubtedly the weakest aspect of the calculation. In general, the coarse vertical resolution artificially destabilizes the shorter wavelength normal modes which have very shallow vertical structure. One may therefore be confident that these calculations at least set upper bounds on the growth rates of any instability.

Some baroclinic instability was present around the plateau edge. Its development was inhibited by the slope of the lower boundary. In any case, the vertical shear was small, implying weak growth rates. All the modes were small scale and extremely shallow, with the largest eddy fluxes confined to the lowest 15 kPa of the atmosphere. The maximum growth rate was 0.12 day^{-1}. The further addition of modest surface friction was enough to stabilize all modes.

More vigorous instability was obtained with a modified basic zonal flow shown in Fig. 5. This was again generated by the axisymmetric model, but included a surface temperature increase of 30 K at 60°S. This increase was included to model the temperature contrast between the ice-covered polar sea and the ice-free parts of the lower latitude Southern Ocean. A stronger jet resulted in this simulation. Most of the vertical shear was associated with this temperature contrast at the ice edge, although it was enhanced by the drainage flow. In this case a maximum growth rate (with friction included) of 0.58 days^{-1} was obtained, with a zonal wavelength of 2400 km. The modes were very shallow, essentially confined below 70 kPa (the approximate level of the summit plateau). The temperature flux was poleward at the lowest levels, and decreased rapidly with height. The momentum fluxes in contrast were mainly equatorward, and decreased

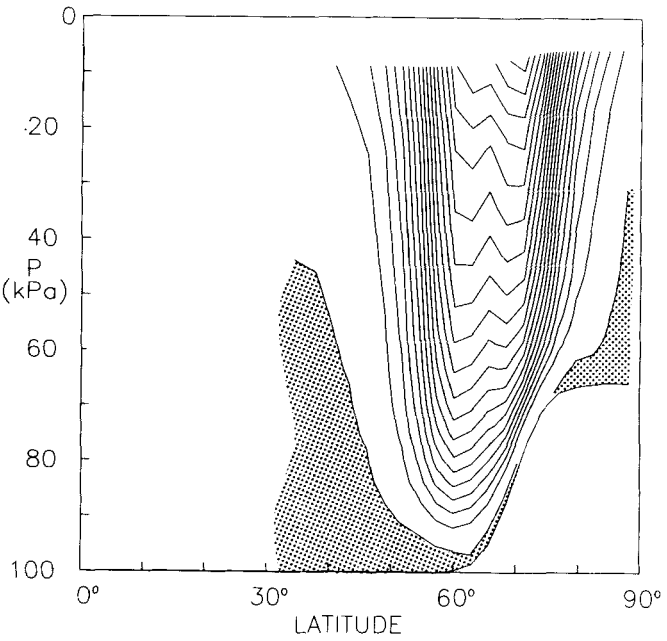

Fig. 5. Latitude-pressure cross-section of the zonal wind generated by the primitive equation model with an increase of surface temperature by 30 K equatorward of 60°. Contour interval 1 ms^{-1}, easterlies shaded.

rapidly with height. The circulations induced by these fluxes involve a good deal of cancellation, although the indirect circulation driven by the temperature fluxes will dominate. Some weak descent, and hence downslope surface wind, might be generated poleward of the baroclinic zone. But the shallowness of the modes means that they can do little to weaken the circumpolar vortex at upper levels. They will not therefore release substantial drainage flow.

Small-scale cyclones are observed around the periphery of Antarctica (J. Turner, personal communication 1989). They are shallow systems and latent heat release may play an important role in their development. It is not yet clear whether their distribution is local or widespread. In any event, their shallow structure implies that they will not make very large contributions to the upper level vorticity budget.

The classic life-cycle simulations (Simmons & Hoskins 1978) for mid-latitude cyclones demonstrate a deepening and considerable enhancement of the momentum fluxes in the nonlinear phase of the life-cycles. This is associated with strong upward and then equatorward propagation of wave activity during this phase of the development (Edmon *et al.* 1980). Such strong developments are considered unlikely for the circumpolar disturbances described here. The weak potential vorticity gradients at high latitudes preclude the vertical propagation of such small-scale disturbances, and so it is expected that the entire life-cycle will be confined to low levels, with the induced circulation not deviating much from the pattern suggested by the linear normal modes.

In conclusion, local baroclinic instability seems unlikely to strengthen the drainage flow significantly.

https://doi.org/10.1017/S0954102089000404 Published online by Cambridge University Press

Gravity wave drag

It has recently been shown that the breaking of orographically forced gravity waves in the upper troposphere may be an important component of the upper tropospheric momentum budget, at least in the Northern Hemisphere winter (Palmer *et al.* 1987, MacFarlane 1987). Many general circulation and numerical weather prediction models now incorporate a parametrization of 'gravity wave drag' based on a simple linear theory of the forcing, vertical propagation and breaking of gravity waves. Current models predict rather little gravity wave drag over Antarctica, despite the very large subgrid scale variance of the orography near the edge of the ice sheet. On the other hand, Mobbs & Rees (1989) report evidence of substantial gravity wave drag, up to 10 ms^{-1} day^{-1}, in the lower troposphere in the vicinity of Halley station on the Brunt Ice Shelf. It is not surprising that simple linear formulations break down; the typical height variance around the Antarctic periphery exceeds the depth of the inversion layer, while as the Ekman analysis showed, the wind vector may turn through as much as 120° through the surface inversion layer.

If the results of Mobbs & Rees (1989) can be generalized to many parts of the plateau edge, then the gravity waves drag could play an important role in weakening the circumpolar vortex. and therefore in maintaining the surface drainage flow. A deceleration of the westerly flow with a maximum in the upper troposphere would introduce a dipole source term into equation (29), negative below the level of the maximum drag and positive above. This will induce a thermally direct circulation below the breaking level and an indirect circulation above.

Internal evidence from general circulation models about the effect of their ability (with or without gravity wave drag) to simulate the drainage flow is conflicting. Recent preliminary results of the UK Universities, Global Atmospheric Modelling Project (UGAMP) model show a remarkably realistic drainage flow. Results from a UK Meteorological Office GCM show a more disorganised and weaker drainage flow (C.A. Senior & J.F. Mitchell, personal communication 1988). This matter requires further study and it is planned to report upon it in due course.

Decaying mid-latitude cyclones

Depression systems generated in the Southern Hemisphere storm track tend to spiral polewards towards the end of their life cycle. Physick (1981) noted certain 'graveyard' regions for depressions around the periphery of Antarctica, which are associated with the climatological low pressure centres observed in the Weddell Sea, Prydz Bay and Ross Sea regions. The decaying depression is typically an equivalent barotropic, cyclonic vortex, which has little phase tilt with height but which is most intense near the tropopause.

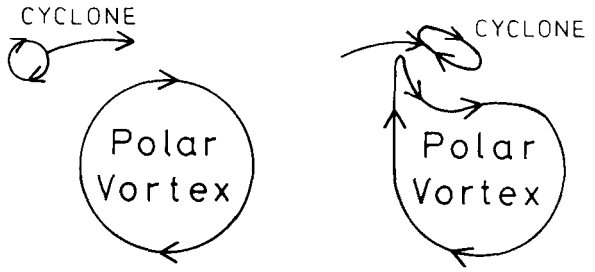

Fig. 6. Schematic illustration of the interaction between a decaying mid-latitude cyclone and the polar vortex.

As such a vortex approaches the main circumpolar vortex, there will be a strong interaction. The circulation induced by the depression will shear the circumpolar vortex, pulling streamers of high cyclonic vorticity air out into lower latitudes. Mid-latitude air, with generally less cyclonic vorticity, will spread into the polar regions. Thus a net flux of cyclonic vorticity out of the circumpolar vortex will be induced. Fig. 6 shows a schematic view of the process. In terms of the linear, quasi-geostrophic theory which has been referred to earlier in this section, the decaying cyclone may be thought of as a fairly small scale (large wave number) packet of Rossby waves. The poleward propagation implies (from equation (30)) that l is negative; from equation (32) there must therefore be a large equatorward flux of westerly momentum, as we require.

This is an attractive hypothesis for the maintenance of the surface drainage winds for several reasons. Unlike baroclinic instabilities or propagating Rossby waves, the flux will be substantial at upper tropospheric levels, and could easily balance the generation of vorticity by the drainage flow. Furthermore, the process is likely to be dominated by a small number of major events, suggesting a degree of sporadicity in the drainage wind. This is of course just what is observed, especially near the coast. Periods of strong drainage flow alternate with periods of calm, leading to a moderate time mean drainage flow. These periods would vary across the continent as the large-scale pressure pattern associated with the approaching mid-latitude vortex passes over the undulations of the ice sheet.

This hypothesis can be tested easily, since both general circulation models and operational analyses for numerical weather prediction should resolve the systems concerned adequately. It is planned to explore this hypothesis by using a simple barotropic model, and by diagnosis of both ECMWF data and the results of the UGAMP model. These diagnostics will be reported in due course.

Conclusions

The strong surface cooling characteristic of the Antarctic ice sheet in winter sets up a pattern of drainage winds which may be qualitatively described in terms of buoyancy driven

https://doi.org/10.1017/S0954102089000404 Published online by Cambridge University Press

Ekman layers. This diabatic circulation extends through the depth of the troposphere, and sets up a strong polar vortex on a timescale of a few days. The results predicted by a classic analytical Ekman layer model have been confirmed using a primitive equation numerical model with very simple frictional and diabatic processes but sophisticated dynamics.

The flow predicted by the model is broadly in agreement with the flow predicted by Egger's (1985) model. That is, there is easterly motion in the boundary layer, with westerly flow above throughout the depth of the troposphere. The major difference is the absence of the strong low level jet which Egger produced near the ice edge. Strong vertical shear is of course expected in that vicinity because of the strong horizontal temperature gradients at the ice edge. But the reasons for the decrease of wind above 2000 m in Egger's simulation, with its implication of a reversed temperature gradient at these levels, is less clear. It may be connected with the development of a 'hydraulic jump' above the discontinuity of slope at the edge of the ice sheet in Egger's model, an effect which is deliberately omitted from the model described in this paper.

Both models, however, reveal that the drainage wind is not a steady state solution of the equations in an axisymmetric model. As the upper vortex strengthens, so the drainage flow is progressively reduced. Indeed, the final steady state consists of zero drainage flow, with increasing westerlies aloft. The simple Ekman pumping model predicts the same result; the timescale for the damping of the drainage flow is related to the timescale for setting up the upper vortex, since the basic mechanism is the development of a large scale pressure gradient which opposes the downslope component of the buoyancy force. Timescales of a few days are typical.

It was concluded that the observed persistence of the drainage flow over wide areas of the continent must imply mechanisms for reducing the cyclonic vorticity over the polar cap at upper levels. This may either be a local friction which can destroy the vorticity *in situ*, or it may involve export of cyclonic vorticity to lower latitudes. The export of cyclonic vorticity by interactions between the polar vortex and decaying mid-latitude systems is proposed as the most likely mechanism.

The downslope drainage winds are a special feature of Antarctica which may have implications for the flow on the entire Southern Hemisphere. The drainage acts to centre the polar vortex over Antarctica; in so doing, it generates a wave number 1 disturbance which dominates the winter mean flow at least as far north as 40°S (James 1988). The simple models reported in this paper give a qualitative account of the dynamical processes involved, although they do not model the details of the boundary layer structure very accurately. The independence of the basic results concerning the surface wind speed and direction of K and τ suggests that such detail may be of only secondary importance to the large scale drainage pattern. It is concluded that the gross features of the middle and upper tropospheric response to the surface drainage flow may not be sensitive to the details of the boundary layer structure.

A logical next step in this work will be to carry out detailed diagnostics of the circulation at high southern latitudes as simulated by the UGAMP global circulation model. This model apparently reproduces the gross features of the drainage flow. The vorticity budget above Antarctica in the model will reveal whether local friction or vorticity fluxes induced by mid-latitude cyclones balance the source of cyclonic vorticity implied by the observed surface drainage winds.

Acknowledgments

This work was funded by the British Antarctic Survey (BAS) as part of their first Antarctic Special Topic programme. I am grateful to BAS for their support, particularly those individuals at BAS who generously offered advice and encouragement. I would especially record my thanks to Mr D.W.S. Limbert. I am grateful to Mr K. Dunn who assisted in the computing. J. Egger, C. Mechoso and I. Watterson are thanked for their helpful discussions.

References

Ball, F.K. 1960. Winds on the ice slopes of Antarctica. *Antarctic meteorology: proceedings of the symposium, Melbourne 1959*. New York: Pergamon, 9–16.

Edmon, H.J., Hoskins, B.J. & McIntyre, M.E. 1980. Eliassen-Palm cross sections for the troposphere. *Journal of Atmospheric Science*, **37**, 2600–2616.

Egger, J. 1985. Slope winds and the axisymmetric circulation over Antarctica. *Journal of Atmospheric Science*, **42**, 1859–1867.

Hoskins, B.J. & Simmons, A.J. 1975. A multi-layer spectral model and the semi-implicit method. *Quarterly Journal of the Royal Meteorological Society*, **101**, 637–655.

James, I.N. 1988. On the forcing of planetary scale Rossby waves by Antarctica. *Quarterly Journal of the Royal Meteorological Society*, 619–637.

James, I.N. & Hoskins, B.J. 1985. Some comparisons of atmospheric internal and boundary baroclinic instability. *Journal of Atmospheric Science*, **42**, 2142–2155.

James, I.N. & Gray, L.J. 1986. Concerning the effect of surface drag on the circulation of a baroclinic planetary atmosphere. *Quarterly Journal of the Royal Meteorological Society*, **112**, 1231–1250.

Mahrt L.J. & Schwerdtfeger, W. 1970. Ekman spirals for exponential thermal wind. *Boundary Layer Meteorology*, **1**, 137–145.

MacVean, M.K. & James, I.N. 1986. On the differences between the lifecycles of some baroclinic waves using the primitive and quasi-geostrophic equations on a sphere. *Journal of Atmospheric Science*, **43**, 741–748.

McFarlane, N.A. 1987. The effect of orographically excited gravity wave drag on the general circulation of the lower stratosphere and troposphere. *Journal of Atmospheric Science*, **44**, 328–338.

Mechoso, C. 1980. The atmospheric circulation around Antarctica: linear stability and finite amplitude interactions with migrating cyclones. *Journal of Atmospheric Science*, **37**, 2209–2233.

Mobbs. S.D. & Rees, J.M. 1989. Studies of atmospheric internal gravity waves at Halley station, Antarctica, using radiosondes. *Antarctic Science*, **1**, 65–75.

PALMER, T.N., SHUTTS, G.J. & SWINBANK, R. 1986. Alleviation of a systematic westerly bias in general circulation and numerical weather prediction models through an orographic gravity wave drag parametrization. *Quarterly Journal of the Royal Meteorological Society*, **112**, 1001–1040.

PARISH, T.R. 1982. Surface airflow over east Antarctica. *Monthly Weather Review*, **110**, 84–90.

PARISH, T.R. & BROMWICH, D.H. 1987. The surface wind field over the Antarctic ice sheets. *Nature*, **328**, 51–54.

PHYSICK, W.L. 1981. Winter depression tracks and climatological jet streams in the Southern Hemisphere during the FGGE year. *Quarterly Journal of the Royal Meteorological Society*, **107**, 883–898.

SCHWERDTFEGER, W. 1984. *Weather and climate of the Antarctic*. Amsterdam: Elsevier, 261 pp.

SIMMONS, A.J. & HOSKINS, B.J. 1978. The lifecycles of some baroclinic waves. *Journal of Atmospheric Science*, **35**, 414–432.

WYATT, L.R. 1981. Linear and nonlinear instabillty of the Northern Hemisphere winter zonal flow. *Journal of Atmospheric Science*, **38**, 2121–2129.